Chattering-Free Sliding Mode Control with a Fuzzy Model for Structural Applications

Keyvan Aghabalaei Baghaei*[1], Hosein Ghaffarzadeh[1a], S. Ali Hadigheh[2b] and Daniel Dias-da-Costa[2,3a]

[1]Department of Civil Engineering, University of Tabriz, Tabriz, Iran
[2]School of Civil Engineering, University of Sydney, Sydney, Australia
[3]ISISE, Department of Civil Engineering, University of Coimbra, Portugal

(Received keep as blank , Revised keep as blank , Accepted keep as blank)

Abstract. This paper proposes a chattering-free sliding mode control (CFSMC) method for seismically excited structures. The method is based on a fuzzy logic (FL) model applied to smooth the control force and eliminate chattering, where the switching part of the control law is replaced by an FL output. The CFSMC is robust and keeps the advantages of the conventional sliding mode control (SMC), whilst removing the chattering and avoiding the time-consuming process of generating fuzzy rule basis. The proposed method is tested on an 8-story shear frame equipped with an active tendon system. Results indicate that the new method not only can effectively enhance the seismic performance of the structural system compared to the SMC, but also ensure system stability and high accuracy with less computational cost. The CFSMC also requires less amount of energy from the active tendon system to produce the desired structural dynamic response.

Keywords: sliding mode control; chattering; fuzzy logic; structural control

1. Introduction

Vibration mitigation and structural control have drawn the attention of many researchers over the last decades as an effective method for dissipating vibration energy. The necessity of reducing building vibrations has motivated researchers into developing various control schemes such as active, semi-active, and passive methods, with the first two being proposed more recently. These systems are characterised by adaptive mechanisms in which control forces are generated by employing external power (Yeganeh Fallah and Taghikhany 2014, Askari *et al.* 2016, Marian and Giaralis 2017, Younespour and Ghaffarzadeh 2016).

The active structural control process requires measuring the structural response, determining the force from the measurements, and applying a designed load to obtain the controlled or desired structural response. Adaption to structural changes and environment relies on the algorithm used as a processor in the active control mechanisms, which can strongly impact the performance of the control system. Fisco and Adeli (2011a) carried out a review study on active and semi-active control of structures performed from 1997. In a companion paper, the authors also reviewed variously improved and new control strategies developed for civil structures (Fisco and Adeli 2011b). The key element to achieve a proper control requires selecting an effective control algorithm for obtaining the control force that needs to be applied to the structural system.

The sliding mode control (SMC) method, as a nonlinear algorithm, was introduced to active control of civil structures by Yang *et al.* (1995) and Adhikari and Yamaguchi (1997), and is based on high-frequency switching (Solea and Nunes 2007). The variable structure of the SMC makes it capable of switching between different control laws. Since the SMC is insensitive against changes and external excitation, it has become a competitive choice among other control methods. Several applications can be highlighted (Yu *et al.*, 2016; Yeganeh Fallah and Taghikhany, 2015; Wu and Yang, 2004; Lee and Chen, 2011; Baradaran-nia *et al.*, 2012; Yang *et al.*, 2015).

Even though the SMC has many advantages, the chattering phenomenon associated with the switches in the control force can negatively impact the actuators during the dynamic mitigation and is often pointed out as the major drawback for practical implementation. Various alternatives were proposed to improve the control performance of conventional SMC, for example, based on the boundary layer method (Adhikari and Yamaguchi, 1997), higher order SMC (Ozer *et al.*, 2017), gain adaption (Wang and Adeli, 2012), and neural networks (Yakut and Alli, 2011; Li *et al.*, 2000).

Having into account the current state of knowledge, a different approach is proposed in this paper to achieve a chattering-free SMC. The method is based on a fuzzy logic

*Corresponding author, Graduate Student
E-mail: k.aghabalaei@gmail.com
[a]Associate Professor
[b]Lecturer

model to estimate and replace the discontinuity of the SMC law, i.e., the source of the chattering, by a smoother approximation. Fuzzy logic control (FLC) as a smart control technique has been used for active control in structures (Guclu and Yazici, 2008; Yu et al., 2016; Ghaffarzadeh and Aghabalaei, 2017; Gu et al., 2019). Human knowledge base and less mathematical effort made it a convenient control technique. The method uses an approximation reasoning and applies linguistic statements to the relationship between system variables. In this paper, the CFSMC is applied to a control system based on active tendons. Such system uses pre-stressed cables or diagonal bracings located between floors of a structure or at the ends of cables in cable-stayed bridges that can be activated axially by servo-controlled hydraulic actuators to quickly adjust the stress state. The method proposed in the following sections is validated using a numerical example under earthquake excitations where uncontrolled and controlled responses are analysed.

2. Control System Model

The motion equation for a controlled structural system with n-degrees of freedom can be written as:

$$M\ddot{x}(t) + C\dot{x}(t) + Kx(t) = Bu(t) + MR\ddot{x}_g(t), \qquad (1)$$

where M, C, and K are $(n \times n)$ mass, damping and stiffness matrices, respectively; $\ddot{x}(t)$, $\dot{x}(t)$ and $x(t)$ are the $(n \times 1)$ acceleration, velocity and displacement vectors, respectively; B is a $(n \times r)$ location matrix of r controllers, and R is a $(n \times 1)$ vector denoting the influence of the earthquake excitation $\ddot{x}_g$ with terms equal to -1.

The state space form of Eq. (1) can be expressed as follows:

$$\dot{z}(t) = Az(t) + B_1u(t) + B_2\ddot{x}_g(t), \qquad (2)$$

where

$$A = \begin{bmatrix} o & I \\ -M^{-1}K & -M^{-1}C \end{bmatrix}; \quad B_1 = \begin{bmatrix} o \\ M^{-1}B \end{bmatrix}$$

$$B_2 = \begin{bmatrix} o \\ M^{-1}R \end{bmatrix}; \quad z(t) = \begin{Bmatrix} x(t) \\ \dot{x}(t) \end{Bmatrix},$$

and A is a $(2n \times 2n)$ plant matrix of the system; B_1 is a $(2n \times r)$ control location matrix; B_2 is an excitation influence vector of size $(2n \times 1)$; $z(t)$ is a $(2n \times 1)$ state vector related to the floor displacements and velocities, and $u(t)$ refers to the control law making Eq. (2) solvable.

In this paper, an active tendon configuration is proposed to apply the control force on the structure. Since such system is based on diagonal elements, which already exist in many structures after stiffening and strengthening, it becomes an attractive practical solution. Fig. 1 shows the control mechanism.

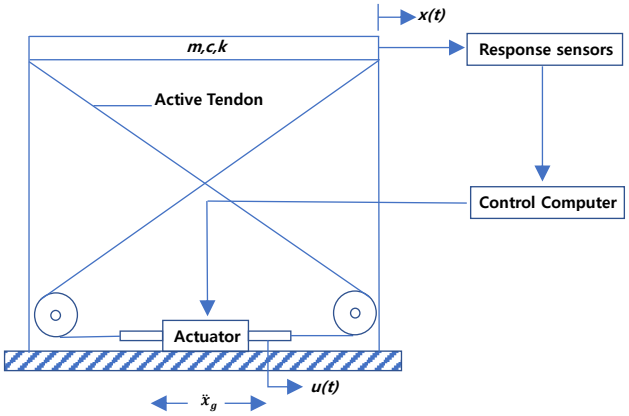

Fig. 1 Active tendon system.

As it is shown in Fig. 1, tendons are installed between two stories. The hydraulic actuator is comprised of an actuator, a servo valve, and a fluid pumping system attached to the lower floor. One end of the tendon is connected to the upper floor and the other end to the piston. The relative movement due to inter-story drift caused by structural vibration alters the tension state of the tendons, which generates a dynamic force to mitigate the response.

3. Sliding Mode Control

The basic strategy of the SMC is based on enforcing the system to move towards a steady state regime by defining a suitable control force. The steady state is known as the sliding switching surface. In the SMC, the structure of the controller is purposely changed by a switching feedback law to drive the trajectories of the controlled system onto the specified sliding surface, known as reaching phase, and enforce them to remain on the surface sliding towards the equilibrium point. Such condition is known as sliding mode (Slotine and Li 1991).

The sliding surface is herein set as a linear function of system states:

$$\sigma(z) = Sz, \qquad (3)$$

where S is the sliding surface coefficient matrix $(r \times 2n)$. A suitable choice of S together with constraint conditions in Eq. (4) leads the trajectories to reach the sliding surface and slide over it.

$$\dot{\sigma}(z) = 0 \quad \text{and} \quad \sigma(z) = 0. \qquad (4)$$

The linear quadratic regulator (LQR) method is used to determine S and design the sliding surface (Yang et al 1995), where the integral of the quadratic function of the state vector is minimised to derive the sliding surface coefficient matrix.

$$J = \int_0^\infty Z(t)^T QZ(t)dt. \qquad (5)$$

In Eq. (5), Q denotes a $(2n \times 2n)$ positive definite diagonal weighting matrix. Using transformation matrix, D, the state

equation and the sliding surface can be written in terms of a transformed state vector Y,

$$Y = DZ; \qquad Z = D^{-1}Y$$
$$D = \begin{bmatrix} I_{2n-r} & -B_1 B_2^{-1} \\ 0 & I_r \end{bmatrix}; \quad B_1 = \begin{bmatrix} B_{11} \\ B_{12} \end{bmatrix}, \tag{6}$$

where I_{2n-r} and I_r are $(2n-r)\times(2n-r)$ and $(r\times r)$ identity matrices, respectively. $B_{11} = (2n-r)\times r$ and $B_{12} = r \times r$ sub-matrices are obtained from the partition of B_1 in Eq. (2). Hence,

$$\dot{Y} = \bar{A}Y + \bar{B}U; \quad \sigma = \bar{S}Y = 0, \tag{7}$$

in which

$$\bar{A} = DAD^{-1}; \quad \bar{S} = SD^{-1}; \quad \bar{B} = \begin{bmatrix} 0 \\ B_{12} \end{bmatrix}. \tag{8}$$

The performance index J defined earlier then becomes:

$$J = \int_0^{\infty} [Y_1', Y_2']\, T \begin{bmatrix} Y_1 \\ Y_2 \end{bmatrix} dt, \tag{9}$$

where Y_1 and Y_2 are $(2n-r)$ and r vectors, respectively, and

$$T = \left[(D^{-1})' Q D^{-1}\right]; \quad T = \begin{bmatrix} T_{11} & T_{12} \\ T_{21} & T_{22} \end{bmatrix}. \tag{10}$$

T_{11} and T_{22} are $(2n-r)\times(2n-r)$ and $(r\times r)$ matrices, respectively, and by minimising Eq. (9), S can be obtained from Eq. (8) as $S = \bar{S}D$.

To calculate the control law, Eq. (2) is replaced into $\dot{\sigma}(z) = 0$ as follows:

$$\dot{\sigma}(z) = S\dot{z} = S(Az + B_1 u + B_2 \ddot{x}_g) = 0, \tag{11}$$

$$u_{eq} = -(SB_1)^{-1}(SAz + SB2\ddot{x}_g). \tag{12}$$

Since the earthquake excitation is not known beforehand, the control law in Eq. (12) cannot be directly used, and the disturbance $(B_2\ddot{x}_g)$ has to be neglected. To account for the earthquake excitation and compensate the uncertainties in the disturbances, a discontinuous control law can be obtained via the known system parameters and under appropriate conditions (Slotine and Li 1991). To guarantee the existence and reachability of the sliding mode, the control law can be implemented by the following inequality:

$$\sigma^T(z)\dot{\sigma}(z) < -\eta|\sigma|, \tag{13}$$

where η is a positive constant value. Substituting Eq. (2) into Eq. (13), we get:

$$\sigma^T(z)S(Az + B_1 u + B_2\ddot{x}_g) < -\eta|\sigma|. \tag{14}$$

Considering $u(t)$ as:

$$\begin{aligned} u(t) &= -(SB_1)^{-1}SAz - (\eta+\gamma)\, sgn(\sigma^T SB_1)^T \\ &= u_{eq} - (\eta+\gamma)\, sgn(\sigma^T SB_1)^T, \end{aligned} \tag{15}$$

where γ is the bound on excitation vector, and sgn stands for the sign function, Eq. (14) can be written as:

$$\begin{aligned} \sigma^T\dot{\sigma} &= \sigma^T(SAz - SB_1[(SB_1)^{-1}SAz \\ &\quad -(\eta+\gamma)\, sgn(\sigma^T SB_1)^T] + SB_2\ddot{x}_g) \\ &= \sigma^T\left(-SB_1(\eta+\gamma)\, sgn(\sigma^T SB_1)^T + SB_2\ddot{x}_g\right) \\ &= -\eta|\sigma^T SB_1| - \gamma|\sigma^T SB_1| + \sigma^T SB_2\ddot{x}_g \\ &= -\eta|\sigma^T SB_1| - \gamma|\sigma^T SB_1|\left(1 - \frac{\sigma^T SB_2\ddot{x}_g}{\gamma|\sigma^T SB_1|}\right) \\ &< -\eta|\sigma^T SB_1|. \end{aligned} \tag{16}$$

Therefore, considering $u(t)$ given by Eq. (15) and satisfying Eq. (13) guarantees the existence and reachability of a sliding mode. For $K = \eta + \gamma$, the control law can finally be rewritten as:

$$u = u_{eq} - K\, sgn(\sigma^T SB_1)^T. \tag{17}$$

Fig. 2 illustrates the block diagram of the SMC. However, the direct implementation of Eq. (15) causes the chattering phenomenon due to the discontinuous part of the equation $(sgn(\sigma SB_1))$ which frequently changes the sign of the control force within a short time periods generating high-frequency switches.

Chattering can be reduced by introducing a continuous approximation of the discontinuous sliding mode controller within a thin boundary layer neighbouring the sliding surface to smooth switches. One possible mathematical form of such solution is based on the replacement of the sign function with a term derived from the fuzzy inference mechanism as discussed in the next section.

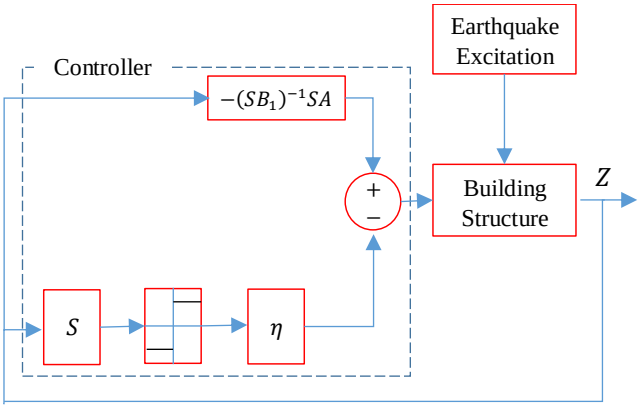

Fig. 2 Block diagram of SMC.

4. Chattering-Free Sliding Mode Control

Among various techniques available to reduce chattering, the boundary layer method can approximate the sign function in Eq. (15) by using a saturation function. Accordingly, a thin boundary layer is defined in the neighbourhood of the sliding surface where chattering occurs. Fig. 3 indicates the schematic view of the chattering phenomenon and the boundary layer neighbouring the sliding surface.

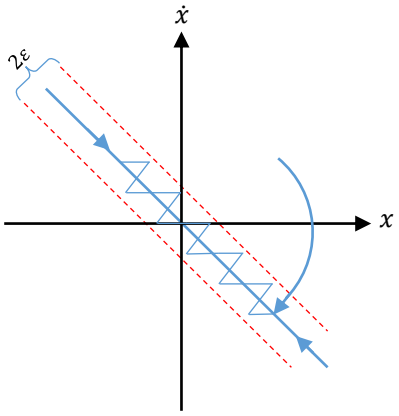

Fig. 3 Sliding surface with chattering and boundary layer.

The saturation function is written as follows:

$$sat(\sigma/\varepsilon) = \begin{cases} \sigma/\varepsilon & \text{if} |\sigma/\varepsilon| \leq 1 \\ sgn(\sigma/\varepsilon) & \text{otherwise} \end{cases} \quad (18)$$

where ε is a positive constant and 2ε is the thickness of the boundary layer. This method smooths the control signal by estimating and replacing the sign function with the saturation function illustrated in Fig. 4.

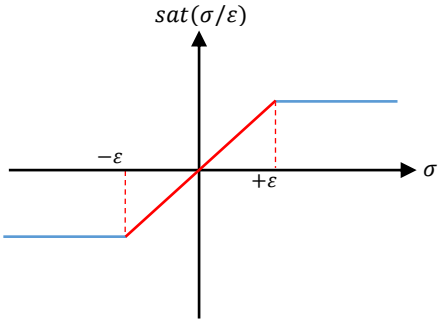

Fig. 4 Linear approximation of the sign function.

The method, however, creates the loss of accuracy in the control signal. In this paper, a different approach is proposed based on a fuzzy inference system to estimate the discontinuous part of Eq. (15) and smooth the control signal. Fig. 5 shows a typical fuzzy logic system.

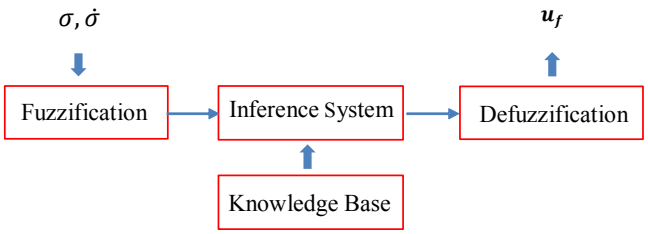

Fig. 5 Structure of a fuzzy logic system.

The step of fuzzification converts crisp inputs into fuzzy sets and allocates a degree of membership to every fuzzy input value between 0 and 1. Each fuzzy set can make use of different types of membership functions such as triangular, trapezoidal, and Gaussian. The knowledge base unit consists of IF-THEN rules, each comprising antecedent and consequent propositions. A fuzzy rule based on SMC can be written as:

$$IF \underbrace{\sigma \text{ is } A_1 \text{ and } \dot{\sigma} \text{ is } A_2}_{(1)} \text{ THEN } \underbrace{u_f \text{ is } B}_{(2)},$$

where σ is a switching variable, $\dot{\sigma}$ stands for its derivative, u_f is the fuzzy output; and A_i and B are the fuzzy input and output sets, and (1) and (2) represent the statements. The inference system performs fuzzy operations to map the fuzzy inputs to outputs. The defuzzification step maps the fuzzy output in a crisp value for the control law.

To apply the SMC strategy, the fuzzy rules can be obtained based on the trajectories in the phase plane. Specifically, the control force is calculated to bring back the trajectory to a proper state leading to the desired control action. The fuzzy rules can be explained with respect to the various positions and directions of trajectories and without any trial and error as in conventional rule bases.

Table 1 shows the fuzzy rule base, where P, N, L, M, S, Z means Positive, Negative, Large, Medium, Small, Zero, respectively. The symbols represent linguistic values of $\sigma, \dot{\sigma}$, and u_f. For example, for a position in the trajectory far from the sliding surface and in the positive region ($\sigma = PL$) while moving from it ($\dot{\sigma} = PL$), a considerable control force is needed to restore the trajectory towards the sliding surface ($u_f = NL$).

Table 1 Knowledge base of fuzzy SMC.

$\dot{\sigma}/\sigma$	PL	PM	PS	Z	NS	NM	NL
PL	NL	NL	NM	NS	NS	Z	Z
PM	NL	NM	NM	NS	Z	Z	PS
PS	NM	NM	NS	NS	Z	PS	PS
Z	NM	NS	NS	Z	PS	PS	PM
NS	NS	NS	Z	PS	PS	PM	PM
NM	NS	Z	Z	PS	PM	PM	PL
NL	Z	Z	PS	PS	PM	PL	PL

The proper choice of membership functions can lead to the most suitable approximation of sign functions. In this study, Gaussian and singleton type membership functions are used for input and output fuzzy members, respectively. Moreover, by using singleton fuzzification, product inference, and center-average defuzzification, the fuzzy output can also be obtained as (Hsiao *et al*. 2005):

$$u_f = \frac{\sum_{j=1}^{m} w_j c_j}{\sum_{j=1}^{m} w_j} = v^T \psi, \quad (19)$$

where

$$w_j = \prod_{i=1}^{n} \mu_{F_i^j}(x_i); \quad v = [c_1, \ldots, c_m]^T, \quad (20)$$

$$\psi = \frac{[w_1 \quad \dots \quad w_m]^T}{\sum_{j=1}^{m} w_j}. \tag{21}$$

In Eqs. (19)-(21), m and n are the total number of fuzzy rules and input variables, respectively; c_j represents the center of the membership function in the consequent part of the j-th rule; $\mu_{F_i^j}(x_i)$ denotes the membership value of the linguistic variable x_i to the fuzzy set F_i in the j-th rule; w_j represents the firing strength of the j-th rule; and ψ is the firing strength vector.

Based on the fuzzy control rules for $\sigma \neq 0$, the fuzzy control output (u_f) enforces the system trajectories to return to the sliding surface, which is in fact identical to the SMC inequality law, i.e., $\sigma(z)\dot{\sigma}(z) < 0$. Using the fuzzy model and replacing the sign function with u_f then fulfills the reachability and existence of a sliding mode.

The new control method can handle different control actions based on the different states of σ and $\dot{\sigma}$, which implies a nonlinear mapping from σ and $\dot{\sigma}$ to u_f. Hence, the chattering-free SMC (CFSMC) law can be written as shown in Eq. (22), and the nonlinear approximation of the sign function within the boundary layer in the neighbourhood of the sliding surface takes the shape illustrated in Fig. 6.

$$\begin{aligned} u_{CFSMC} &= u_{eq} - (\eta + \gamma)\, sgn(\sigma^T S B_1)^T \\ &= u_{eq} - K(u_f). \end{aligned} \tag{22}$$

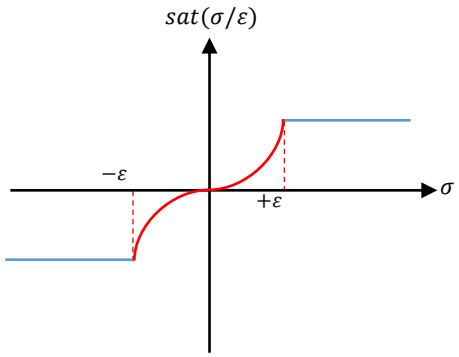

Fig. 6 Fuzzy approximation of the sign function.

5. Numerical Study

A numerical example based on an eight-story shear building equipped with active tendons in the first and the eighth stories is used in this section to illustrate the application of the CFSMC and its effectiveness in avoiding chattering whilst reducing the dynamic responses of all stories. The method is also compared against conventional SMC.

The dynamic properties of the structure selected for analysis are indicated in Table 2 (Yang *et al.* 1995). The earthquake records of El Centro (1940) and Northridge (1994) are used as dynamic excitation, as detailed in Table 3. The acceleration records of the two earthquakes are also depicted in Fig. 7.

Table 2 Mass, stiffness, and damping values of the building.

Story	Mass (ton)	Stiffness (kN/m)	Damping (kN.s/m)
1	345.6	3.4×10^5	490
2	345.6	3.2×10^5	467
3	345.6	2.85×10^5	410
4	345.6	2.69×10^5	386
5	345.6	2.43×10^5	349
6	345.6	2.07×10^5	298
7	345.6	1.69×10^5	243
8	345.6	1.37×10^5	196

Table 3 Properties of selected ground motions.

Earthquake	El Centro	Northridge
Station	Imperial Valley, Station No.117	Alhambra, CA, Fermont School
Magnitude	6.9	6.6
Depth (km)	8.8	18
PGA (cm/s^2)	341.69	99.08
PGV (cm/s)	33.45	10.89
PGD (cm)	10.86	2.47

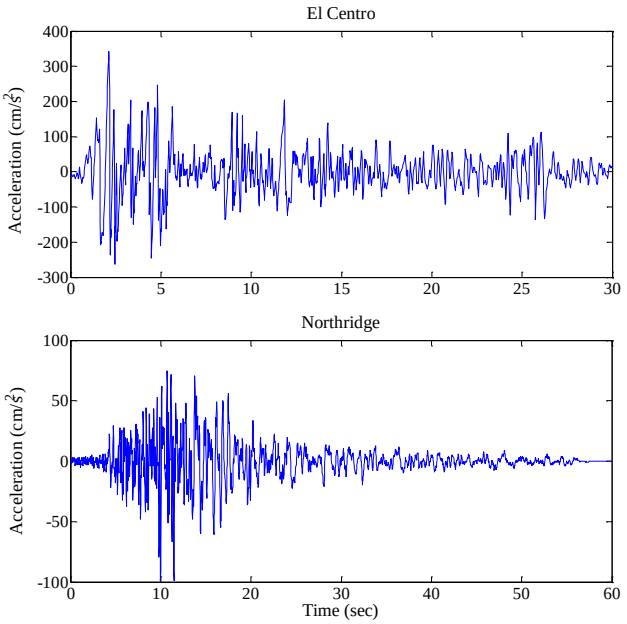

Fig. 7 Time histories of the selected ground motions.

Fig. 8 illustrates the configuration of the building, where due to the significant values of the shear force and displacement in the first and eighth stories, those floors are equipped with the active tendon systems. The standard response time of the actuator is considered between 6-16 milliseconds, in which case the active tendon system can be assumed to produce the desired control force instantly.

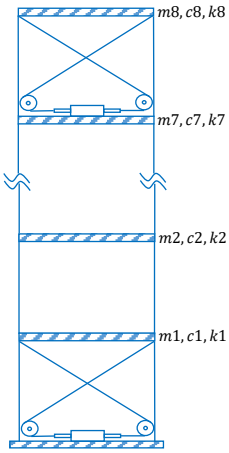

Fig. 8 Structural model of the active tendon system.

With the SMC, the sliding surface is determined with the LQR method using a diagonal weighting matrix Q where $Q_{ii} = 10^6$ for i=1, 2, ..., 8, and $Q_{ii} = 1$ for i=9, 10, …, 16. For the configuration of the active tendon system shown in Fig. 8 with a 45° inclination angle, the sliding surface equation for the controller in the first floor becomes:

$$\sigma_1 = 709.206(z_1) - 278.298(z_2) - 498.556(z_3) + 31.819(z_4) - 20.578(z_5) - 17.553(z_6) - 9.142(z_7) - 4.444(z_8) + 90.214(z_9) + 89.211(z_{10}) + 52.61(z_{11}) + 37.889(z_{12}) + 28.719(z_{13}) + 19.434(z_{14}) + 12.165(z_{15}) + 6.082(z_{16}).$$

For the controller installed on the eighth floor, the corresponding sliding surface equation is given by:

$$\sigma_8 = 4.444(z_1) + 4.286(z_2) + 22.001(z_3) + 46.535(z_4) + 29.971(z_5) - 4.206(z_6) - 160.228(z_7) + 709.206(z_8) + 6.745(z_9) + 6.745(z_{10}) + 7.132(z_{11}) + 8.497(z_{12}) + 10.567(z_{13}) + 10.629(z_{14}) + 29.409(z_{15}) + 15.498(z_{16}).$$

The FLC model is also designed using two input variables (σ and $\dot{\sigma}$) and one output variable (u_f) each with seven membership functions. The functions chosen for both input and output variables are gaussian-shaped and singleton functions, respectively, as shown in Fig 9. Therefore, the fuzzy model is constructed with 49 rules. The values of v are obtained according to the fuzzy control rules set in Table 1. Finally, it should be mentioned that K is considered as 200 for both SMC and CFSMC laws.

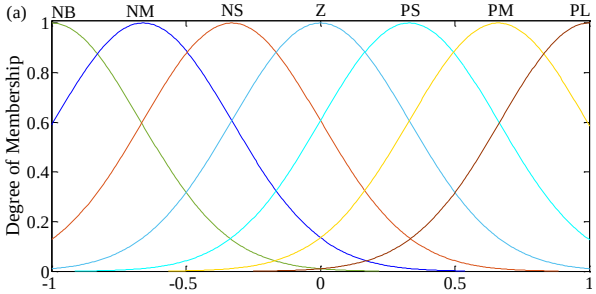

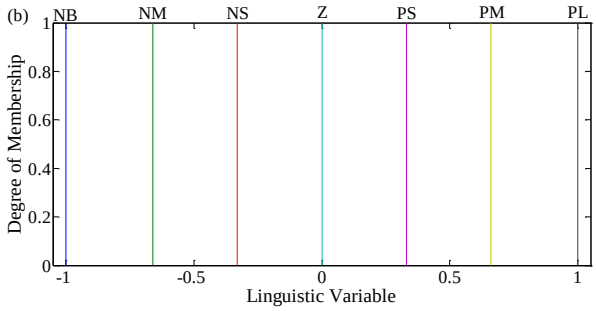

Fig.9 Membership functions: (a) input variables ($\sigma, \dot{\sigma}$); (b) output variable (u_f).

Fig. 10 shows the uncontrolled and controlled displacements with the SMC and CFSMC for the first and the eighth stories during the El Centro excitation. From Fig. 10 it can be concluded that both methods can decrease the displacements considerably.

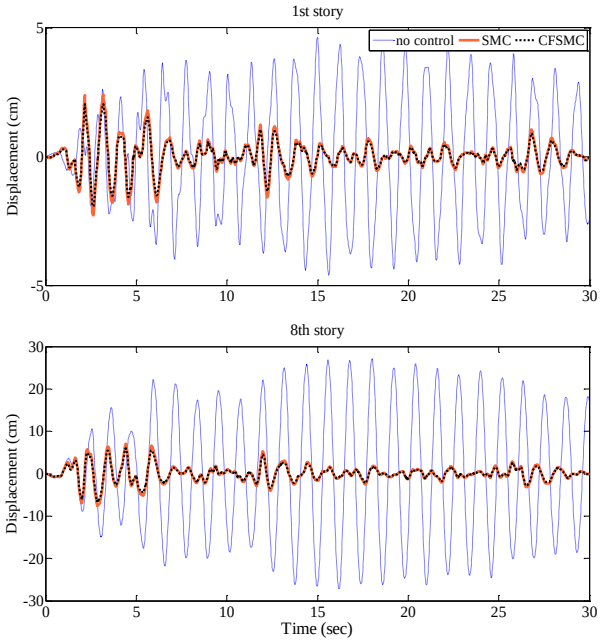

Fig.10 Displacement responses during El Centro earthquake.

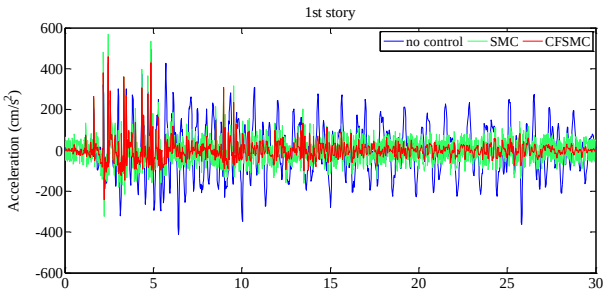

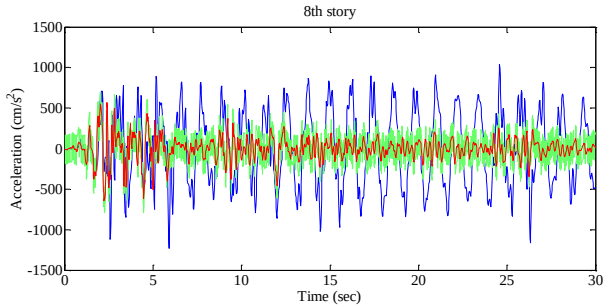

Fig.11 Acceleration responses during El Centro earthquake.

The acceleration responses are depicted in Fig. 11, where the high-frequency switches obtained with the SMC method is evident. During the Northridge earthquake, both control methods demonstrated a good performance (Fig. 12). However, the high-frequency switches prevent the SMC to reduce the acceleration responses satisfactorily (Fig. 13).

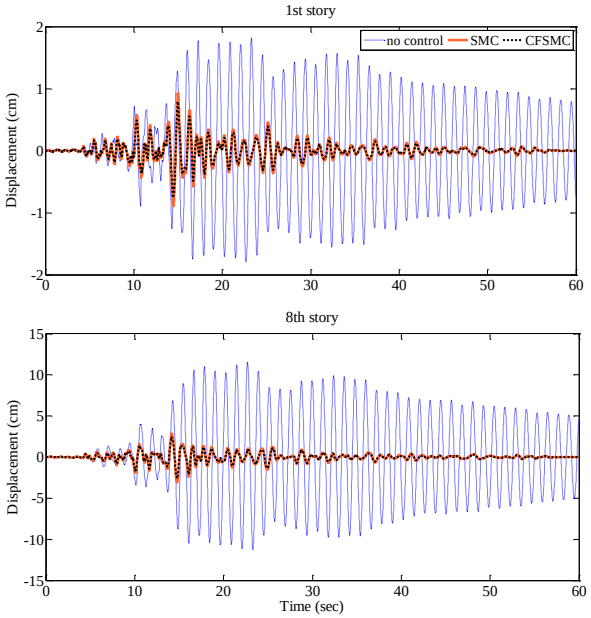

Fig.12 Displacement responses during Northridge earthquake.

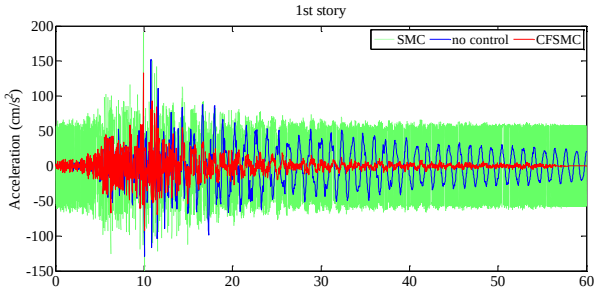

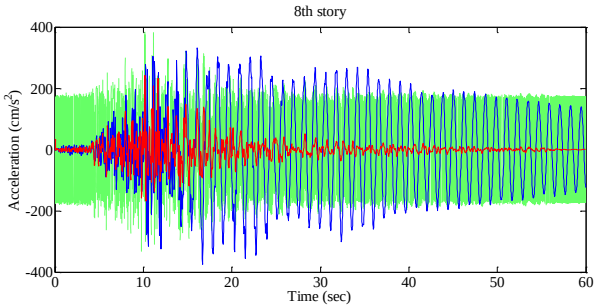

Fig.13 Acceleration responses during Northridge earthquake.

To better illustrate the chattering phenomenon in the conventional SMC, the time histories for the control forces are represented in Figs. 14 and 15 for both floors. Considerable switches are present in the time histories of the control forces with the SMC which can lead to reduced control accuracy and high wear of moving mechanical parts, thus preventing the actuators to generate the desired control force in a non-simulated situation.

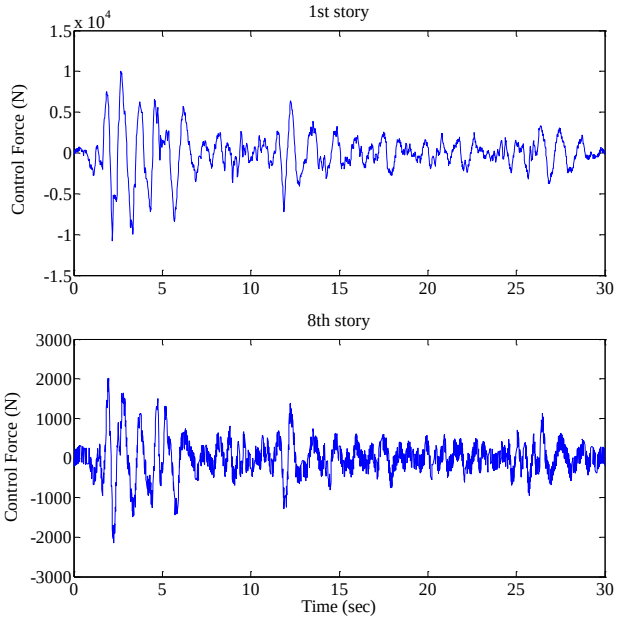

Fig. 14 Control force with SMC during El Centro earthquake.

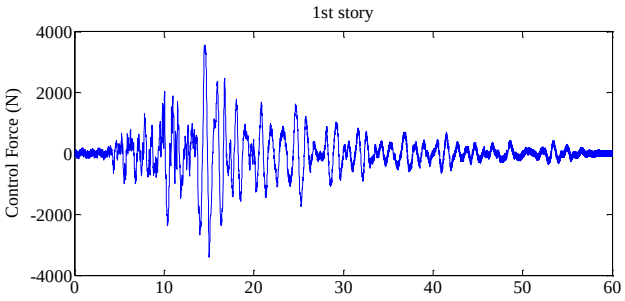

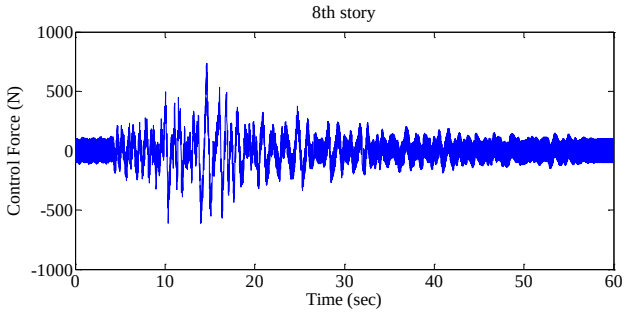

Fig. 15 Control force with SMC during Northridge earthquake.

Fig. 16 shows the forces for first and eighth stories during the El Centro excitation with the CFSMC, whereas Fig. 17 shows the same output for the Northridge excitation. Comparison with Figs. 14 and 15 allows concluding that chattering is effectively eliminated with the CFSMC due to the replacement of the sign function with the fuzzy output without losing accuracy. The maximum response quantities registered during both earthquakes – see Tables 4 and 5 – are also significantly smaller with the CFSMC.

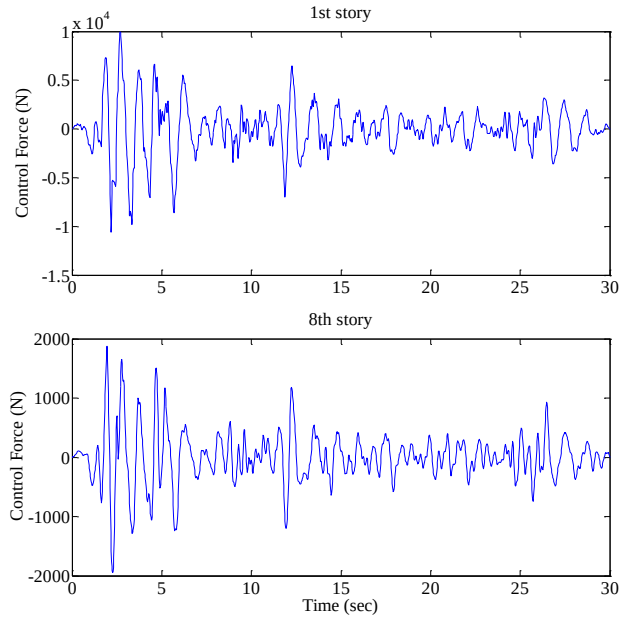

Fig. 16 Control force with CFSMC during El Centro earthquake.

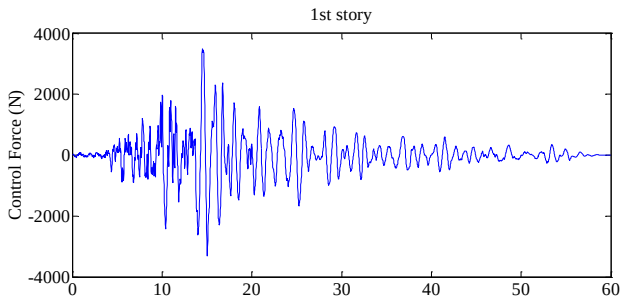

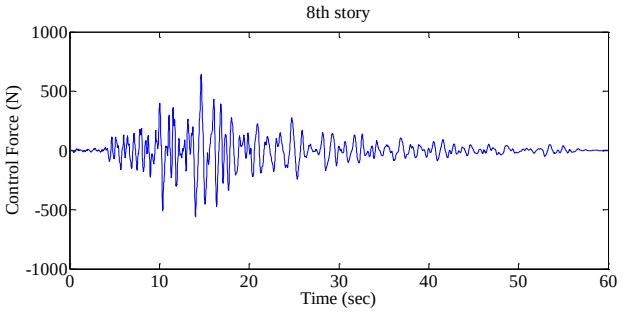

Fig. 17 Control force with CFSMC during Northridge earthquake.

Table 4 Maximum response quantities during El Centro earthquake.

	Story	No control	SMC	CFSMC
$x\ (cm)$	1	4.63	2.41	2.41
	8	27.16	7.48	7.48
$\ddot{x}\ (cm/s^2)$	1	496	568	459
	8	1,230	792	643
$U\ (N)$	1	-	10,790	10,587
	8	-	2,141	1,940

Table 5 Maximum response quantities during Northridge earthquake.

	Story	No control	SMC	CFSMC
$x\ (cm)$	1	1.81	0.93	0.93
	8	11.56	3.1	3.1
$\ddot{x}\ (cm/s^2)$	1	152	191	133
	8	375	385	241
$U\ (N)$	1	-	3,660	3,492
	8	-	839	641

The performance of the control system given by the root mean square (RMS) of uncontrolled and controlled responses for both SMC and CFSMC methods is represented in Figs. 18 and 19. Even though the displacement responses in both approaches are identical, the chattering negatively impacts the RMS values obtained with the SMC, which is evident in Fig. 19.

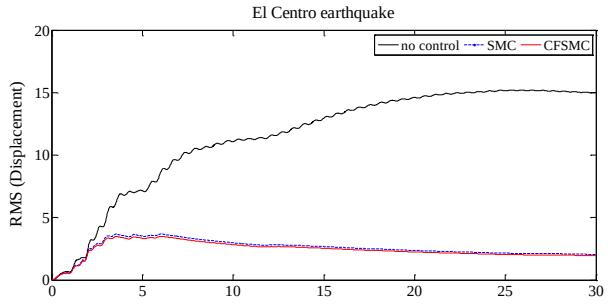

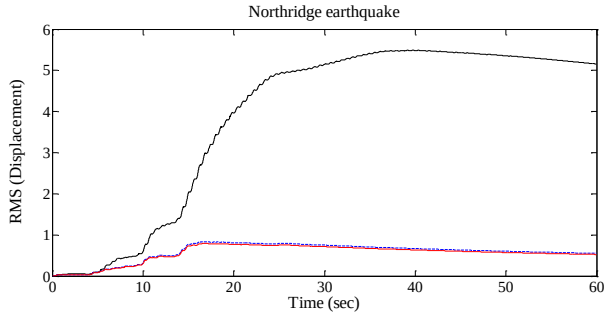

Fig. 18 RMS of displacements.

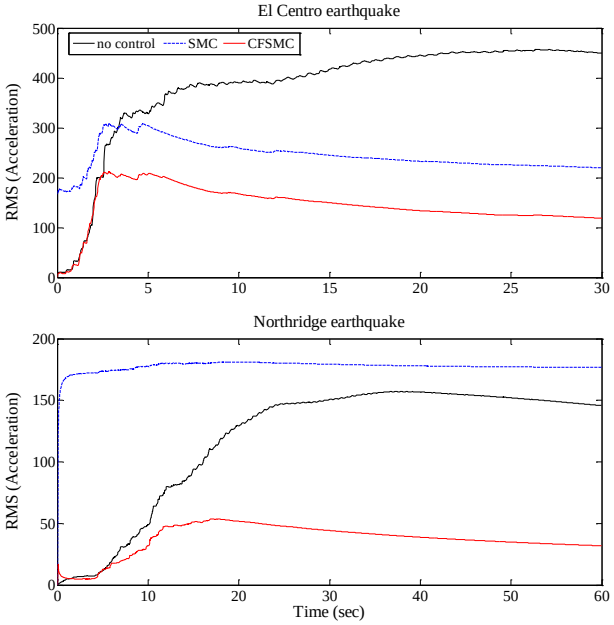

Fig. 19 RMS of accelerations.

Finally, an indication about the energy consumption of the control method can be derived from the RMS for the control forces as shown in Fig. 20. The CFSMC requires smaller forces to achieve suitable dynamic performance in comparison to the SMC. The proposed method not only reduces the dynamic responses with less amount of energy consumption, but also removes chattering in the actuator, which could cause a control system malfunction in practical applications.

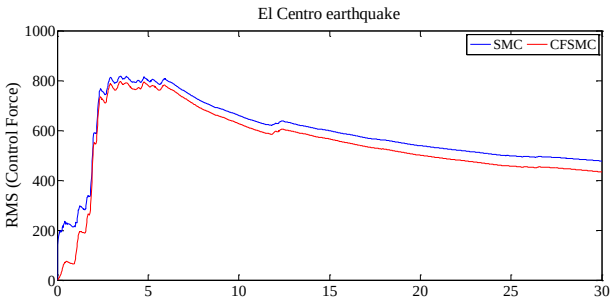

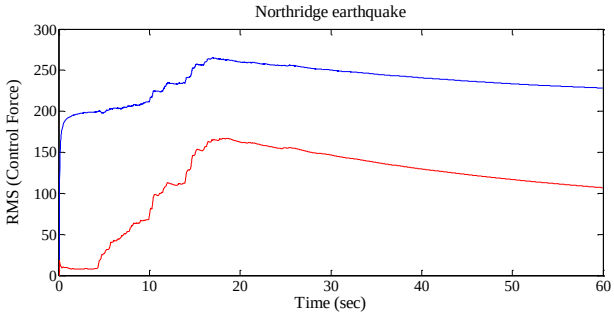

Fig. 20 RMS of control forces.

6. Conclusions

A chattering-free sliding mode control (CFSMC) methodology is presented in this paper to improve the performance of the conventional SMC. The proposed approach takes advantage of a fuzzy model for designing a chattering-free SMC effectively avoiding excessive switches. Moreover, using the concept of the sliding mode for constructing the fuzzy rules basis, a trial-and-error process is avoided. To validate the proposed method, the CFSMC was employed to reduce the seismic responses of an 8-story building equipped with an active tendon system. Results demonstrate the performance of the proposed method against the SMC to eliminate chattering with high accuracy, whilst reducing the dynamic responses. It was demonstrated that the CFSMC is an effective strategy for enhancing the performance of the conventional method in seismic isolation of structures.

While this study focussed on the dynamic response of structures due to seismic excitation, some important issues will remain and require further studies to fully assess the proposed control strategy, such as the stability analysis, nonlinearity, and uncertainty in the structural properties. The proposed method could also be extended to time-delay problems and structures with material deterioration under strong excitations.

Acknowledgements

Dias-da-Costa would like to acknowledge ARC grants DE150101703 and LP140100591.

References

Adhikari, R. and Yamaguchi, H. (1997), "Sliding mode control of buildings with ATMD", *Earthquake Engineering and Structural Dynamics*, **26**(4), 409-422.

Askari, M., Li, J. and Samali, B. (2016), "Semi-active control of smart building-MR damper systems using novel TSK-Inv and max-min algorithms", *Smart Structures and Systems,* **18**(5), 1005-1028.

Baradaran-nia, M., Alizadeh, G., Khanmohammadi, S. and Farahmand Azar, B. (2012), "Optimal sliding mode control of single degree-of-freedom hysteretic structural system",

Communications in Nonlinear Science and Numerical Simulation, **17**(11), 4455-4466.

Fisco, N.R. and Adeli, H. (2011a), "Smart structures: Part I-active and semi-active control", *Scientia Iranica*, **18**(3), 275–284.

Fisco, N.R. and Adeli, H. (2011b), "Smart structures: Part II-hybrid control systems and control strategies", *Scientia Iranica*, **18**(3), 285–295.

Ghaffarzadeh, H. and Aghabalaei, K. (2017), "Adaptive fuzzy sliding mode control of seismically excited structures", *Smart Structures and Systems,* **19**(5), 577-585.

Gu, X., Yu, Y., Li, Y., Li J., Askari, M. and Samali, B. (2019), "Experimental study of semi-active magnetorheological elastomer base isolation system using optimal neuro fuzzy logic control", *Mechanical Systems and Signal Processing,* **119**, 380-398.

Guclu, R. and Yazici, H. (2008), "Vibration control of a structure with ATMD against earthquake using fuzzy logic controllers," *Journal of Sound and Vibration*, **318**(1-2), 36-49.

Hsiao, F.H., Chen, C.W., Liang, Y.W., Xu, S.D. and Chiang. W.L. (2005), "T-S fuzzy controllers for nonlinear interconnected systems with multiple time delays", *T. Circuits Syst. I: Regular Papers*, **25**(9), 1883-1893.

Lee, T.Y. and Chen, P.C. (2011), "Experimental and analytical study of sliding mode control for isolated bridges with MR dampers", *Journal of Earthquake Engineering*, **15**(4), 564-581.

Li, Z., Deng, Z. and Gu, Z. (2010), "New sliding mode control of building structure using RBF neural networks", *Chinese Control and Decision Conference,* Suzhou, China.

Marian, L. and Giaralis, A. (2017), "The tuned-mass-damper-inerter for harmonic vibrations suppression, attached mass reduction, and energy harvesting", *Smart Structures and Systems,* **19**(6), 665-678.

Ozer, H.O, Hacioglu, Y. and Yagiz, N. (2017), "Controlling the building model using high order sliding mode control optimized by multi objective genetic algorithm", *Periodicals of Engineering and Natural Sciences,* **5**(3), 256-262.

Slotine, J.J.E. and Li, W. (1991), *Applied Nonlinear Control*, Prentice-Hall, Inc., Englewood Cliffs, N.J.

Solea, R. and Nunes, U. (2007), "Trajectory planning and sliding-mode control based trajectory-tracking for cybercars", *Integrated Computer-Aided Engineering*, **14**(1), 33-47.

Wang, N. and Adeli, H. (2012), "Algorithms for chattering reduction in system control", *Journal of the Franklin Institute,* **394**(8), 2687-2703.

Wu, J.C. and Yang, J.N. (2004), "Modified sliding mode control for wind-excited benchmark problem", *Journal of Engineering Mechanics*, **130**(4), 499-504.

Yakut, O. and Alli, H. (2011), "Neural based sliding mode control with moving sliding surface for the seismic isolation of structures", *Journal of Vibration and Control,* **17**(14), 2103-2113.

Yang, J.N., Wu, J.C. and Agrawal, A.K. (1995), "Sliding mode control for nonlinear and hysteretic structures", *Journal of Engineering Mechanics*, **121**(12), 1330-1339.

Yang, T.Y., Li, K., Lin, J.Y., Li, Y. and Tung, D.P. (2015), "Development of high-performance shake tables using the hierarchical control strategy and nonlinear control techniques", *Earthquake Engineering and Structural Dynamics,* **44**(11), 1717-1728.

Yeganeh Fallah, A. and Taghikhany, T. (2014), "Robust semi-active control for uncertain structures and smart dampers", *Smart Materials and Structures,* **23**(9).

Yeganeh Fallah, A. and Taghikhany, T. (2015), "A modified sliding mode fault tolerant control for large-scale civil infrastructures", *Computer Aided Civil and Infrastructure Engineering,* **31**, 550-561.

Younespour, A. and Ghaffarzadeh, H. (2016), "Semi-active control of seismically excited structures with variable orifice damper using block pulse functions", *Smart Structure and Systems,* **18**(6), 1111-1123.

Yu, Y., Royel, S., Li, J., Li, Y. and Ha, Q. (2016), "Magnetorheological elastomer base isolator for earthquake response mitigation on building structures: modeling and second-order sliding mode control", *Earthquake and Structures,* **11**(6), 943-966.

Yu, Y., Li, Y., Li, J., Gu, X., Royel, S. and Pokhrel, A. (2016), "Nonlinear and hysteretic modeling of magnetorheological elastomer base isolator using adaptive neuro-fuzzy inference system", *Applied Mechanics and Materials,* **846**(6), 258-263.